CHAPTER VI
ETHYLENE EPOXIDATION IN A LOW-TEMPERATURE CORONA DISCHARGE SYSTEM: EFEECT OF SEPARATE ETHYLENE/OXYGEN FEED

(Being Prepared for International Journal of Chemical Engineering and Processing: Process Intensification)

6.1 Abstract

In this work, the ethylene epoxidation performance in a low-temperature corona discharge system was improved by initially producing oxygen free radicals prior to react with unactivated ethylene molecules, in which the ethylene was separately fed into the system at various feed positions of the plasma zone. In addition, various operating parameters, including O_2/C_2H_4 feed molar ratio, applied voltage, input frequency, total feed flow rate, and gap distance between pin and plate electrodes, were optimized for the separate feed system. The highest EO yield was achieved under the operating conditions of a C_2H_4 feed position of 0.2 cm, an O_2/C_2H_4 feed molar ratio of 1:2, an applied voltage of 18 kV, an input frequency of 500 Hz, a total feed flow rate of 100 cm^3/min, and an electrode gap distance of 10 mm. Comparisons between the separate feed and the mixed feed of C_2H_4 and O_2 under their own optimum conditions, the separate feed provided higher EO selectivity and yield with lower other product selectivities and lower power, as compared to the mixed feed. The results confirm that the separate feed with a suitable C_2H_4 feed position have a sufficient reaction time with a minimum ethylene molecules to be activated which, in turn, can reduce all undesired reactions including the cracking, dehydrogenation, hydrogenation, combustion, and coupling reactions of ethylene, resulting in superior ethylene epoxidation performance.

Keywords: Epoxidation; Ethylene Oxide; Corona Discharge; Ethylene Feed Position

6.2 Introduction

Non-thermal plasma is a kind of electric gas discharge which has been extensively used in many applications such as chemical reaction processes [1-6], surface modifications [7-9], production of hydrogen and syngas [10-14], decomposition of hydrogen sulfide (H_2S) [15-17], production of hydrogen and elemental sulfur [18], decontamination of air and water streams from chemical pollutants [19], and bio-medical application [20]. The highly energetic discharges or the plasmas are generated from two electrodes which are applied with high voltage to overcome the potential barrier of metal surface electrodes. The generated electrons can collide with reactant molecules in the plasma zone to directly transform to various chemically excited or dissociated gaseous species which can result in subsequential reactions. An interesting characteristic of the non-thermal plasma is its very low bulk gas temperature (close to room temperature), while the generated electron temperature remains a much high temperature (approximately 10^4-10^5 K) [21]. Hence, several chemical reactions, which normally occur at high temperatures, can be forced to occur at ambient temperature and atmospheric pressure, leading to low energy requirement and solving some problems from high temperature operation of the catalytic processes such as deactivation, coke formation, and sintering of catalysts. Therefore, this technique is considered to have a potential to substitute catalytic chemical processes including ethylene epoxidation. Ethylene epoxidation is one of important petrochemical reactions in which the combined catalytic-plasma processes as well as the sole plasma systems have recently been developed as an alternative to the conventional catalytic processes [3-5,22,23].

Ethylene oxide (EO, C_2H_4O) is commercially produced by the selective oxidation of ethylene, called ethylene epoxidation. It is widely used in the petrochemical industry to produce various useful chemicals such as ethylene glycol, detergents by process called ethoxylation, sterilants for foodstuffs, medical equipment, and supplies, solvents, antifreezes, adhesives, and cosmetics [24]. In industry, ethylene is selectively oxidized to EO with high selectivity by using silver catalysts supported on low-surface-area alpha-alumina (Ag/(LSA)α-Al_2O_3). Alkali and transition noble metals, especially cesium (Cs), copper (Cu), rhenium (Re), and

gold (Au) were proved to exhibit the improvement of the EO selectivity as well as halogen promoters such as dichloroethane ($C_2H_4Cl_2$) and vinyl chloride (C_2H_3Cl) [22,25-31]. However, the conventional catalytic processes still provide low ethylene and oxygen conversions and require high operational pressure and temperature, causing high energy consumption and several operational problems including deactivation of catalysts.

The corona discharge, for the first time, was employed to produce EO by our research group [4]. The results showed that the ethylene-to-oxygen ratio significantly influenced ethylene epoxidation performance. However, significant amounts of undesired other products were also produced, resulting from most of ethylene molecules to be activated by the collision of generated electrons. A suitable ethylene feed position was hypothesized in this study that it could provide unactivated ethylene molecules to directly react with generated oxygen active species, leading to improvement of EO production as well as suppression of undesired reactions including cracking, dehydrogenation, hydrogenation, coupling, and CO formation.

In this study, ethylene epoxidation performance was, for the first time, improved using an AC corona discharge system by initially producing oxygen active species prior to reacting with inactivated C_2H_4, which was achieved by using a separate feed of C_2H_4 at various positions along the plasma zone. The effects of various operating parameters, including ethylene feed position, O_2/C_2H_4 feed molar ratio, applied voltage, input frequency, total feed flow rate, and electrode gap distance, on the activity of ethylene epoxidation were also examined.

6.3 Experimental

6.3.1 Reactant Gases

All gases used in this work: 99.995% helium (high purity grade), 40% ethylene balanced with helium (± 1% uncertainty), and 97% oxygen balanced with helium (± 1% uncertainty), were specially blended by Thai Industrial Gas (Public) Co., Ltd. The 30% ethylene oxide in helium (± 1% uncertainty) was used as a

standard gas to obtain the calibration curve of gas chromatography (GC) for EO analysis.

6.3.2 Corona Discharge System

The ethylene epoxidation experiments were performed by using a corona discharge reactor, which was operated at atmospheric pressure and ambient temperature, around 25–27 °C. The schematic of experimental setup for ethylene epoxidation reaction using the corona discharge system is shown in Figure 6.1(a), and the detailed schematic of the corona discharge reactor is shown in Figure 6.1(b). The reactor comprised of an 11.25-inch-long quartz tube with an outer diameter of 10 mm and an inner diameter of 8 mm, and two electrodes, called pin and plate electrodes. The pin electrode was made of a stainless steel rod having a 1 mm outer diameter whereas the plate electrode had a 7 mm diameter and 1 mm thickness with several holes. Plasma was generated in the gap between pin and plate electrodes, which were located at the center of reactor. The power used to generate plasma was alternating current power, 220 V and 50 Hz, which was transformed to a high voltage current via a power supply unit by three steps. For the first step, the AC input power of 220 V and 50 Hz was transformed to a DC output of 70 V by a DC power supply converter. Next, the AC with a sinusoidal waveform and different frequencies was generated from the DC input by a 500 W power amplifier with a function generator. For the third step, the outlet voltage from the second step was stepped up by using a high voltage transformer. The output voltage and frequency were adjusted by the function generator, whereas the sinusoidal waveform was monitored by an oscilloscope. Since the generated plasma is non-equilibrium in nature; therefore, the voltage and current at the low-voltage side were measured instead. The high-side voltage and current were then calculated by multiplying and dividing the measured values by a factor of 130, respectively.

6.3.3 Reaction Activity Experiments

Firstly, the experiments were run under base conditions [4]: an O_2/C_2H_4 feed molar ratio of 0.5:1, an applied voltage of 15 kV, an input frequency of 500 Hz, a total feed flow rate of 100 cm^3/min, and an electrode gap distance of 1 cm at different C_2H_4 feed positions (distance between the plate electrode and C_2H_4 feed

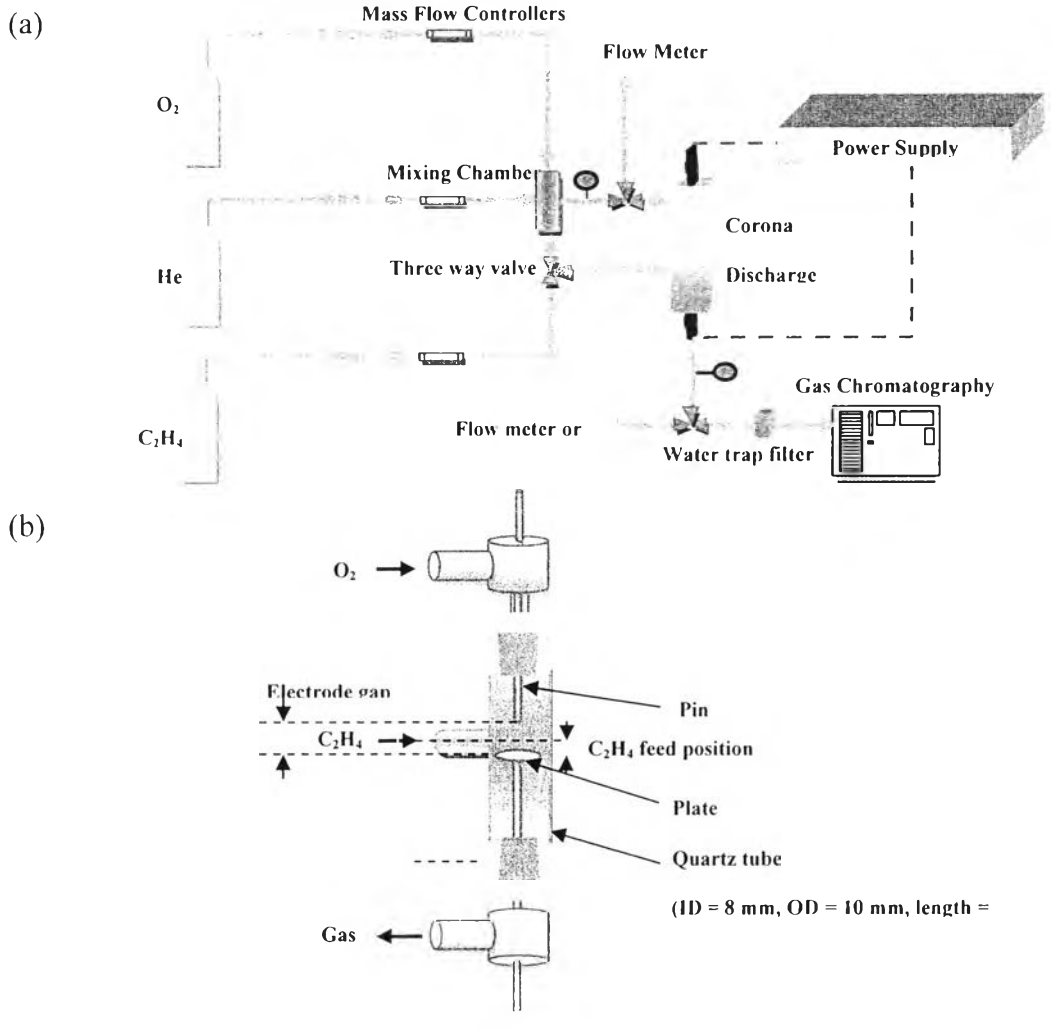

Figure 6.1 (a) Schematic of experimental setup for ethylene epoxidation reaction using a corona discharge reactor and (b) detailed schematic of corona discharge reactor.

point) in order to determine the effect of C_2H_4 feed position on ethylene epoxidation reaction. The C_2H_4 feed position was varied by moving both electrodes up or down while the electrode gap distance was kept constant at 1 cm. The flow rates of C_2H_4, O_2, and helium flowing through the reactor were controlled by electronic mass flow controllers. All reactant gases were trapped by 7-μm in-line filters to remove any solid particles before passing through the electronic mass flow controllers. The reactor pressure was controlled by a needle valve behind the plasma reactor to maintain 1 atmosphere, and the gaseous outlet was either vented to the atmosphere via an exhausted rubber tube or entered an on-line gas chromatograph (Perkin-Elmer,

AutoSystem GC). The moisture in the product gas stream was trapped by a water trap filter before entering the on-line gas chromatograph. The gas chromatograph was equipped with both a thermal conductivity detector (TCD) and a flame ionization detector (FID). For the TCD channel, a packed column (Carboxen 1000) was used for separating hydrogen (H_2), oxygen (O_2), carbon monoxide (CO), and carbon dioxide (CO_2). For the FID channel, a capillary column (OV-Plot U) was used for analysis of ethylene oxide (EO) and other hydrocarbon gases. For any experimental run, the oxygen balanced with helium was fed downward throughout the plasma reactor, whereas the ethylene was injected separately to the plasma zone at different feed positions (Figure 6.1(b)). When the composition of the reactant gases (oxygen and ethylene) in the outlet gas had been invariant with time, the power supply was turned on to generate plasma. The product gas was analyzed by the on-line gas chromatography every 20 min after the system reached steady state. The experimental data with a standard deviation of less than 5% were averaged and then used to assess the plasma system performance in terms of ethylene and oxygen conversions, ethylene oxide selectivity and yield, selectivities for other products, including H_2, CO, CO_2, CH_4, C_2H_6, C_2H_2, and C_3, and power consumption. The conversions, product selectivities and EO yield were defined as:

$$\% \text{ Reactant conversion} = \frac{(\text{moles of reactant in} - \text{moles of reactant out}) \times 100}{(\text{moles of reactant in})} \quad (6.1)$$

$$\% \text{ Product selectivity} = \frac{[(\text{number of carbon atom in product})(\text{moles of product produced})] \times 100}{[(\text{number of carbon atom in ethylene})(\text{moles of ethylene converted})]} \quad (6.2)$$

$$\% \text{ EO yield} = (\% \text{ ethylene conversion}) \times (\% \text{ EO selectivity}) \times 100 \quad (6.3)$$

To determine the energy efficiency of the plasma system, the power consumption was calculated in a unit of Ws per molecule of converted ethylene or per molecule of produced ethylene oxide using Eq.6.4:

$$\text{Power consumption} = \frac{P \times 60}{N \times M} \quad (6.4)$$

where P = Power (W)

N = Avogadro's number = 6.02 X 10^{23} molecules/mol

M = Rate of converted ethylene molecules in feed or rate of produced ethylene oxide molecules (mol/min).

6.4 Results and Discussion

6.4.1 Effect of C_2H_4 Feed Position

The effect of C_2H_4 feed position was initially studied in order to obtain the most suitable C_2H_4 feed position for the ethylene epoxidation reaction. In this work, the C_2H_4 feed position was investigated in the range of 1–7 mm, while the other operating parameters were fixed at an O_2/C_2H_4 feed molar ratio of 0.5:1, an applied voltage of 15 kV, an input frequency of 500 Hz, a total feed flow rate of 100 cm^3/min, and a gap distance between pin and plate electrodes of 1 cm, which were the optimum conditions for the mixed C_2H_4/O_2 feed obtained from our previous work [4]. Under the studied conditions, the shortest C_2H_4 feed position that could generate EO was 1 mm, while there was no EO produced at the C_2H_4 feed position lower than the electrode plate. This is because C_2H_4 molecules mostly presented outside the plasma region, causing lowering to be activated by the collision with the high energetic electrons and the generated active oxygen species. When the C_2H_4 feed position was higher than 7 mm, the feed pattern approached the mixed feed which was already studied in the previous work [4]. As shown in Figure 6.2(a), the C_2H_4 and O_2 conversions only slightly vary in narrow ranges under the studied C_2H_4 feed position range of 1–7 mm with both minima at the C_2H_4 feed position of 0.2 cm. In contrast, the EO yield tended to increase with increasing C_2H_4 feed position from 1 to 2 mm and then gradually decreased with further increasing C_2H_4 feed position over 2 mm. The results showed that at the optimum C_2H_4 feed position of 2 mm, C_2H_4 molecules could react more selectively with the oxygen free radicals in the plasma zone to produce EO with the highest EO yield and the lowest conversion of both C_2H_4 and O_2.

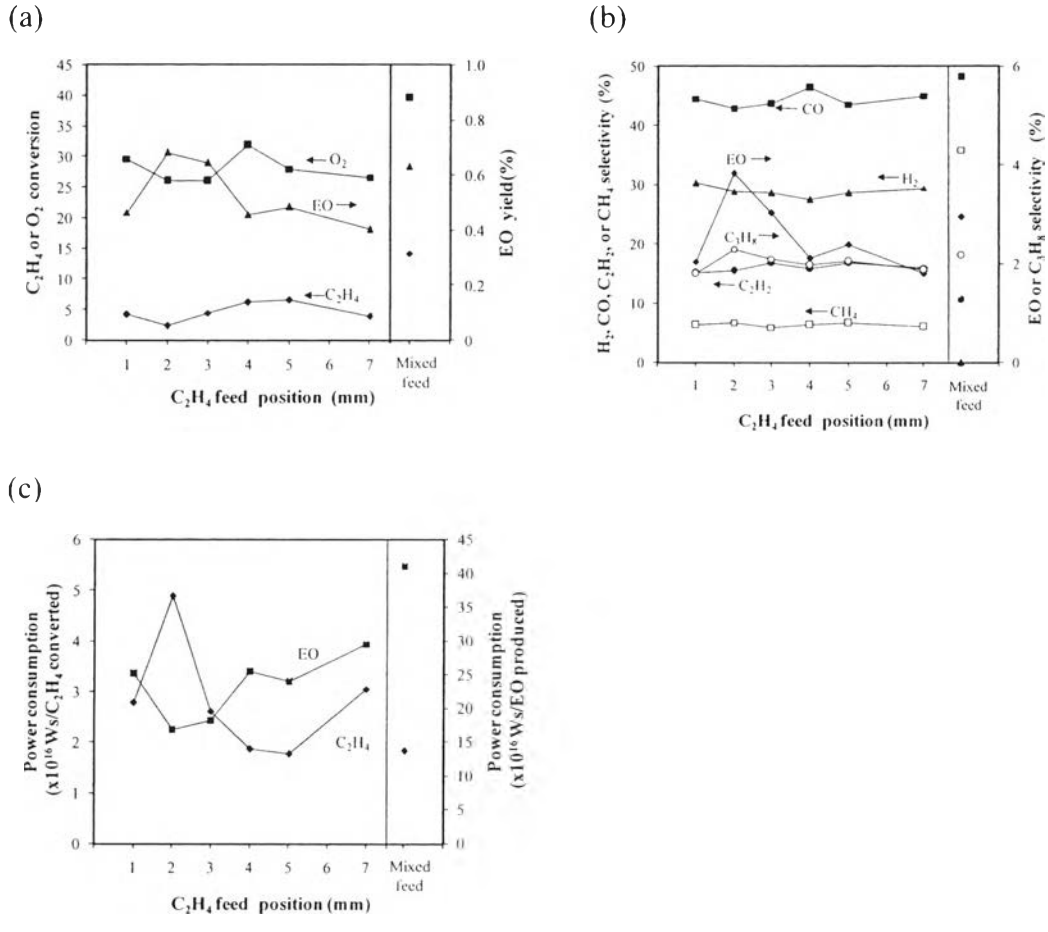

Figure 6.2 (a) C_2H_4 and O_2 conversions and EO yield, (b) product selectivities, (c) power consumption as a function of C_2H_4 feed position (an O_2/C_2H_4 feed molar ratio of 0.5:1, an applied voltage of 15 kV, an input frequency of 500 Hz, a total feed flow rate of 100 cm^3/min, and an electrode gap distance of 1 cm).

Figure 6.2(b) shows the effect of C_2H_4 feed position on the selectivities for EO (desired product), and other products, i.e. CO, H_2, CH_4, C_2H_2, and C_3H_8. The EO, CH_4, and C_3H_8 selectivities tended to increase with increasing C_2H_4 feed position from 1 to 2 mm and then decreased with further increasing C_2H_4 feed position from 0.2 to 0.7 mm, which were in the same trend as the EO yield, whereas the CO, H_2, and C_2H_2 selectivities remained almost unchanged over the entire range of C_2H_4 feed position. The results can be explained by the fact that the opportunity of all reactions between oxygen free radicals and inactivated and

activated C_2H_4 molecules increases with increasing the C_2H_4 feed position because of the increase in C_2H_4 residence time. However, an increase in C_2H_4 feed position directly increases the opportunity of C_2H_4 molecules to be activated by the generated electrones, resulting in increases in undesired reactions in the plasma zone (cracking, CO formation, dehydrogenation, and subsequential coupling). Hence, the system should be operated with a suitable C_2H_4 feed position to maximize the ethylene epoxidation performance with lowest other reactions (details of the proposed mechanisms will be explained later). Interestingly, C_3H_8 was the highest molecular weight hydrocarbon was found with a very small fraction and there was no CO_2 produced because the plasma system was operated under the O_2-lean condition.

Figure 6.2(c) shows the effect of C_2H_4 feed position on the power consumption. The power consumption per molecule of converted C_2H_4 reached a maximum at a C_2H_4 feed position of 2 mm. For a C_2H_4 feed position higher than 2 mm, the power consumption per molecule of converted C_2H_4 rapidly decreased with increasing C_2H_4 feed position. In contrast, there was a rapid decrease in the power consumption per molecule of produced EO with increasing C_2H_4 feed position from 1 to 2 mm, but it increased with further increasing C_2H_4 feed position from 2 to 7 mm. The power consumption per molecule of produced EO was about one order of magnitude higher than that per molecule of converted C_2H_4. The C_2H_4 feed position of 2 mm was considered to be an optimum value and selected for further experiments because it provided the highest EO selectivity, the highest EO yield, and the lowest power consumption per molecule of produced EO.

The ethylene epoxidation activity of the separate C_2H_4/O_2 feed was compared to that of the mixed C_2H_4/O_2 feed which was studied in the previous work [4]. Interestingly, the separate feed could reduce ethylene cracking and combustion reactions, as shown experimentally by extremely lower CH_4 selectivity and comparatively lower CO selectivity, as compared to the mixed feed system. Moreover, the higher EO selectivity and yield were obtained from the separate feed system, especially at the optimum C_2H_4 feed position of 2 mm. In addition, the separate feed system had lower power consumption per molecule of produced EO. However, we hypothesized that the corona system with the separate feed was not yet operated under its own optimum conditions. Therefore, operating conditions, i.e.

O_2/C_2H_4 feed molar ratio, applied voltage, input frequency, total feed flow rate, and electrode gap distance were further investigated in the corona system with the separate feed at the optimum C_2H_4 feed position of 2 mm in order to maximize its process performance toward the ethylene epoxidation reaction.

6.4.2 Effect of O_2/C_2H_4 Feed Molar Ratio

To determine the influence of oxygen content in feed on the ethylene epoxidation reaction under the investigated corona discharge environment, the O_2/C_2H_4 feed molar ratio was varied in the range of 0.25:1–1:1 (O_2-lean conditions), while the other operating parameters were fixed at a C_2H_4 feed position of 2 mm, an applied voltage of 15 kV, an input frequency of 500 Hz, a total feed flow rate of 100 cm^3/min, and an electrode gap distance of 1 cm. The effect of O_2/C_2H_4 feed molar ratio on the C_2H_4 and O_2 conversions and EO yield is shown in Figure 6.3(a). The increase in O_2/C_2H_4 feed molar ratio slightly affected the C_2H_4 conversion, whereas it markedly affected the O_2 conversion. With increasing O_2/C_2H_4 feed molar ratio from 0.25:1 to 0.33:1, the O_2 conversion decreased greatly. The O_2 conversion tended to increase with increasing O_2/C_2H_4 feed molar ratio from 0.33:1 to 0.75:1 and then slightly decreased with further increasing O_2/C_2H_4 feed molar ratio. It can be observed that the O_2 conversion was much higher than the C_2H_4 conversion. This can be explained by the fact that the bond dissociation energy of C_2H_4 (16.7 eV) is higher than that of O_2 (12.2 eV), accordingly causing O_2 molecules to be converted more easily than C_2H_4 molecules. Moreover, the C_2H_4 feed position of 2 mm caused the residence time of C_2H_4 shorter than that of O_2, leading to a lower opportunity of C_2H_4 to be collided with the generated electrons as compared to the feed O_2. It could also be seen that the EO yield tended to increase with increasing O_2/C_2H_4 feed molar ratio from 0.25:1 up to 0.5:1 and then rapidly decreased with further increasing O_2/C_2H_4 feed molar ratio from 0.5:1 to 1:1. These results clearly indicate the significance of the O_2/C_2H_4 feed molar ratio on the ethylene epoxidation performance.

Figure 6.3(b) shows the effect of O_2/C_2H_4 feed molar ratio on all product selectivities. The EO selectivity markedly increased to reach a maximum at an O_2/C_2H_4 feed molar ratio of 0.33:1 and then rapidly decreased with further

increasing O_2/C_2H_4 feed molar ratio from 0.33:1 to 1:1. For the other by-product selectivities, except CO and CH_4, the selectivities for H_2, C_2H_2, and C_3H_8 tended to

(a)

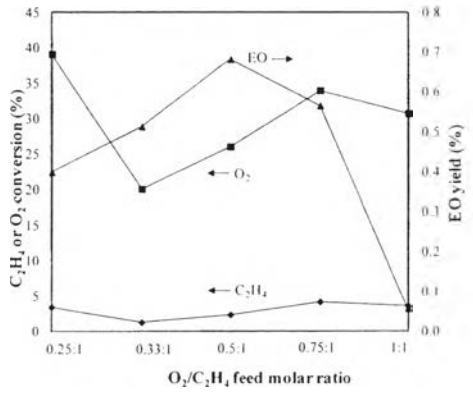

(b)

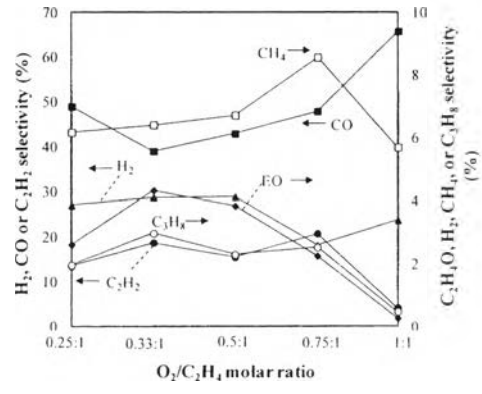

(c)

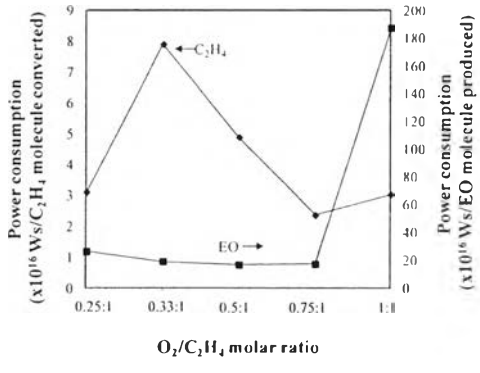

Figure 6.3 (a) C_2H_4 and O_2 conversions and EO yield, (b) product selectivities, (c) power consumption as a function of O_2/C_2H_4 feed molar ratio (a C_2H_4 feed position of 2 mm, an applied voltage of 15 kV, an input frequency of 500 Hz, a total feed flow rate of 100 cm^3/min, and an electrode gap distance of 1 cm).

increase with increasing O_2/C_2H_4 feed molar ratio from 0.25:1 to 0.33:1, and then decreased with further increasing O_2/C_2H_4 feed molar ratio from 0.33:1 to 1:1. The CH_4 selectivity tended to increase with increasing O_2/C_2H_4 feed molar ratio from 0.25:1 to 0.75:1 and then decreased with further increasing O_2/C_2H_4 feed molar ratio higher than 0.75:1. The CO selectivity decreased to reach a minimum at an O_2/C_2H_4 feed molar ratio of 0.33:1 and then increased with further increasing O_2/C_2H_4 feed

molar ratio higher than 0.33:1. The results indicate that the epoxidation reaction to produce EO is more likely to occur under O_2-lean conditions.

The power consumptions required to convert one C_2H_4 molecule and to produce one EO molecule at different O_2/C_2H_4 feed molar ratios are shown in Figure 6.3(c). The power consumption per molecule of converted C_2H_4 reached a maximum at an O_2/C_2H_4 feed molar ratio of 0.33:1, which corresponded well with the lowest C_2H_4 conversion. The power consumption per molecule of produced EO remained almost unchanged in the O_2/C_2H_4 feed molar ratio range of 0.25:1–0.75:1, but then rapidly increased with further increasing O_2/C_2H_4 feed molar ratio from 0.75:1 to 1:1, while the lowest EO selectivity was observed at an O_2/C_2H_4 feed molar ratio of 0.5:1. As mentioned above, the power consumption per molecule of produced EO was much higher than that per molecule of converted C_2H_4 which agrees well with previous studies [3-5,22,23]. The O_2/C_2H_4 feed molar ratio of 0.5:1 was selected for further experiments because it provided the highest EO yield, as well as comparatively low power consumption per molecule of produced EO.

6.4.3 Effect of Applied Voltage

In order to determine the effect of the applied voltage, the reaction experiments were conducted in the applied voltage range of 15–19 kV. The highest applied voltage of 19 kV was limited by the formation of coke filaments between the two electrodes after a relatively short operation period, causing instability and thereby permanent extinction of the plasma. The system could not produce steady plasma when applied voltage was lower than 15 kV. Figure 6.4(a) illustrates the effect of applied voltage on both C_2H_4 and O_2 conversions and EO yield. The O_2 conversion tended to increase significantly with increasing applied voltage in the entire range of 15–19 kV. In contrast, the C_2H_4 conversion remained almost unchanged and was very low throughout the studied range of applied voltage. The explanation for the increased O_2 conversion with increasing applied voltage is that a higher voltage results in a higher generated current, as shown in Figure 6.4(b), which provides higher quantity of electrons to initiate the reactions and brings about greater opportunity for the collision between O_2 molecules and electrons. The very low C_2H_4 conversion can be explained by the fact that the bond dissociation energy of O_2 (12.2

eV) is much lower than that of C_2H_4 (16.7 eV) and the residence time of C_2H_4 lower than that of O_2, causing O_2 molecules to be converted higher than C_2H_4 molecules. Interestingly, the EO yield tended to increase with increasing applied voltage in the range of 15–18 kV and then drastically decreased with further increasing applied voltage beyond 18 kV.

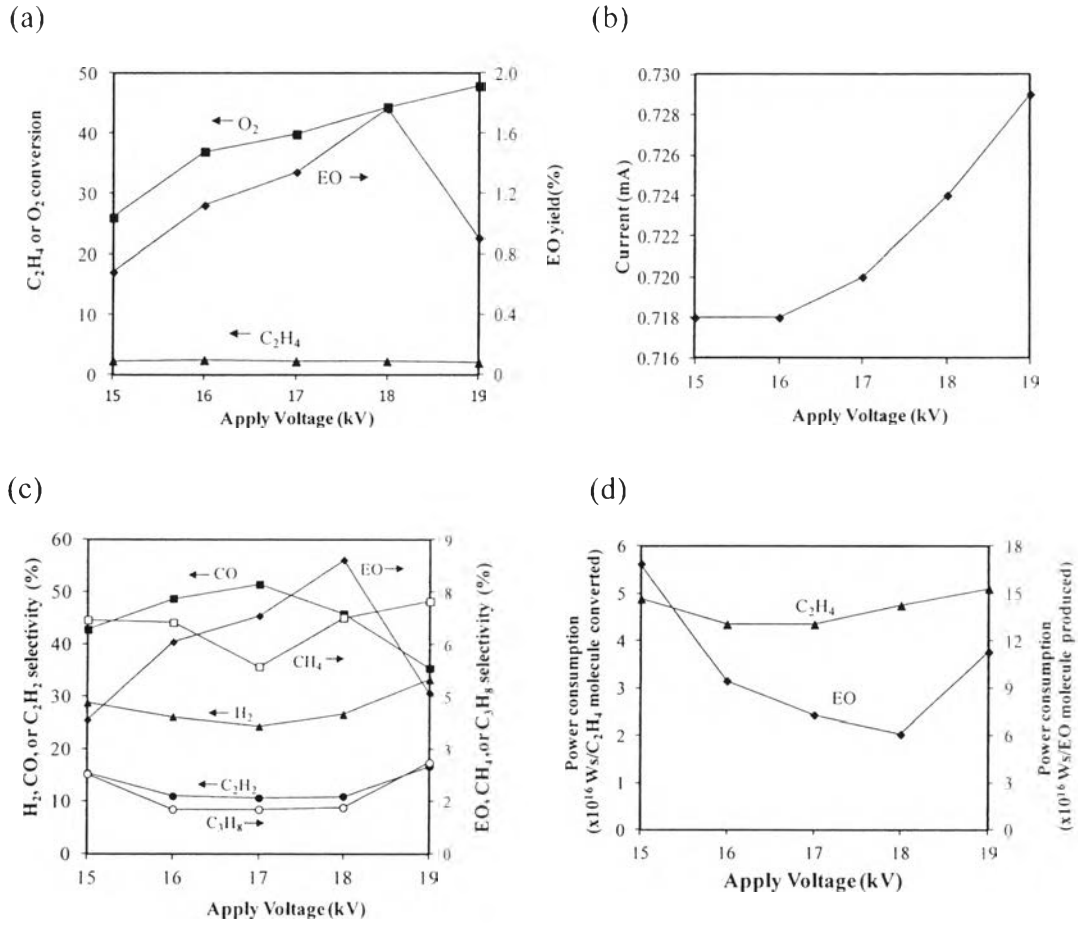

Figure 6.4 (a) C_2H_4 and O_2 conversions and EO yield, (b) generated current, (c) product selectivities, (d) power consumption as a function of applied voltage (a C_2H_4 feed position of 2 mm, an O_2/C_2H_4 feed molar ratio of 0.5:1, an input frequency of 500 Hz, a total feed flow rate of 100 cm^3/min, and an electrode gap distance of 1 cm).

In agreement with the EO yield, the EO selectivity greatly increased with increasing applied voltage in the range of 15–18 kV and then decreased with

further increasing applied voltage beyond the applied voltage of 18 kV (Figure 6.4(c)), possibly due to the earlier explanation for the limitation of coke formation. The selectivities for H_2, CH_4, C_2H_2, and C_3H_8 reached the minimum values at the applied voltage of 17 kV and then increased with further increasing applied voltage from 17 to 19 kV. Interestingly, no CO_2 was detected possibly because the system was operated under the O_2-lean condition (the O_2/C_2H_4 feed molar ratio of 1:2). The CO selectivity increased with increasing applied voltage in the range of 15–17 kV and then decreased with further increasing applied voltage beyond 17 kV. The results can be explained by the fact that an increase in applied voltage simply increases amount of generated electrons, leading to a higher amount of oxygen active species available for reactions with C_2H_4 molecules to yield higher EO selectivity and yield. However, when the system was operated at a very high applied voltage greater than 18 kV, there is a higher opportunity of C_2H_4 to be activated by the high energetic electrons, leading to increases of all undesired reactions (cracking, dehydrogenation, CO formation, and coupling).

The power consumptions needed to convert C_2H_4 molecule and to produce EO molecule at different input frequencies are shown in Figure 6.4(d). The power consumption per molecule of converted C_2H_4 only slightly changed with varying applied voltage, possibly due to the almost unchanged C_2H_4 conversion. On the other hand, the power consumption per molecule of produced EO decreased with increasing applied voltage and reached a minimum at an applied voltage of 18 kV. After that, it increased substantially with further increasing applied voltage beyond 18 kV. From the results, the applied voltage of 18 kV was selected for further investigations because it provided the highest EO yield, the highest EO selectivity, and the lowest power consumption per molecule of produced EO.

6.4.4 Effect of Input Frequency

Input frequency is another important process parameter that greatly affects the plasma characteristics in terms of stability and efficiency performance. The input frequency was experimentally varied in the range of 400–700 Hz. For operating the corona discharge system in this research, the lowest operating input frequency of 400 Hz was limited by a large amount of coke filaments deposited on

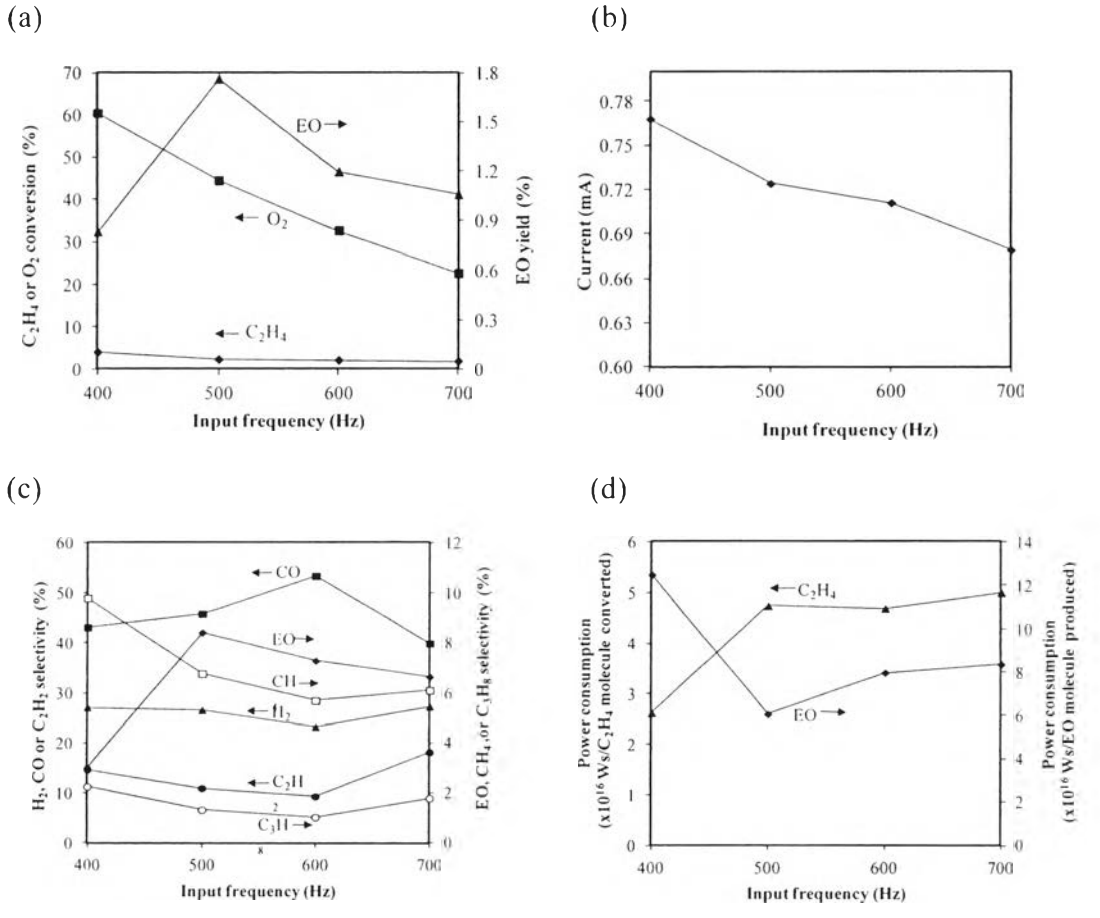

Figure 6.5 (a) C_2H_4 and O_2 conversions and EO yield, (b) generated current, (c) product selectivities, (d) power consumption as a function of input frequency (a C_2H_4 feed position of 2 mm, an O_2/C_2H_4 feed molar ratio of 0.5:1, an applied voltage of 18 kV, a total feed flow rate of 100 cm^3/min, and an electrode gap distance of 1 cm).

the electrode surface, causing unstable plasma with a very high current, whereas the plasma could not exist at an input frequency higher than 700 Hz. The effect of input frequency on the C_2H_4 and O_2 conversions and EO yield is illustrated in Figure 6.5(a). The results show that an increase in the input frequency led to a significant decrease in the O_2 conversion, whereas the C_2H_4 conversion slightly decreased. A possible reason for the decreased O_2 conversion is that an increase in input frequency results in decreasing current, as confirmed in Figure 6.5(b), leading to a lower number of generated electrons and weaker field strength for activating oxygen and C_2H_4 molecules. This subsequently led to lowering conversions of both O_2 and C_2H_4

as well as EO yield at a higher input frequency; however, the EO yield was observed to decrease with decreasing input frequency from 500 to 400 Hz since coke deposition on the electrode surfaces occurred at the lowest input frequency of 400 Hz. The maximum EO yield was found at an input frequency of 500 Hz.

As shown in Figure 6.5(c), the EO selectivity mirrors the EO yield and the maximum EO selectivity was observed at the input frequency of 500 Hz. The CO selectivity slightly increased with increasing input frequency from 400 to 600 Hz and then dramatically decreased with further increasing input frequency from 600 to 700 Hz. For other by-products, their selectivities had an opposite trend to the CO selectivity. This is because a higher frequency gives a lower generated current, resulting in the decrease in amount of oxygen active species for the ethylene epoxidation. However, both EO selectivity and yield decreased remarkably when the input frequency decreased from 500 to 400 Hz. This is because at the input frequency of 400 Hz, the system produces too highly energetic electrons which can further activate C_2H_4 molecules, causing increases in undesired reactions of cracking, dehydrogenation, CO formation, and coupling reactions.

The effect of input frequency on the power consumption to break down each C_2H_4 molecule or to create each EO molecule is shown in Figure 6.5(d). The power consumption per molecule of converted C_2H_4 tended to increase with increasing input frequency; however, the power consumption per molecule of produced EO decreased sharply with increasing input frequency from 400 to 500 Hz and then increased moderately with further increasing input frequency from 500 to 700 Hz. From the results, an input frequency of 500 Hz was considered to be an optimum value because it provided the highest EO yield, the highest EO selectivity, and the lowest power consumption per molecule of produced EO.

6.4.5 Effect of Total Feed Flow Rate

The total feed flow rate has a direct influence on the residence time of gas molecules in the plasma zone, affecting the overall performance of the plasma system. To investigate the effect of total feed flow rate, the experiments were performed by varying total feed flow rate from 100 to 150 cm^3/min. A total feed flow rate lower than 100 cm^3/min was limited by the operation range with high precision

(a)

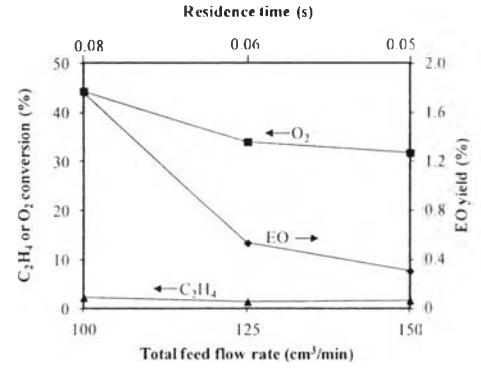

(b)

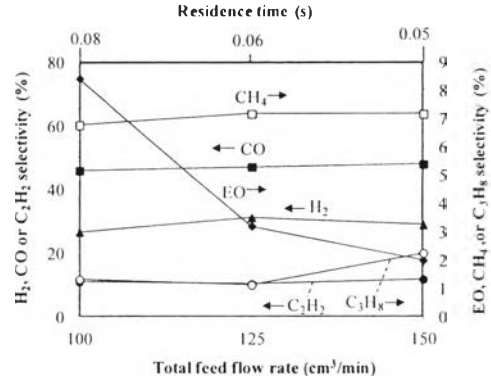

(c)

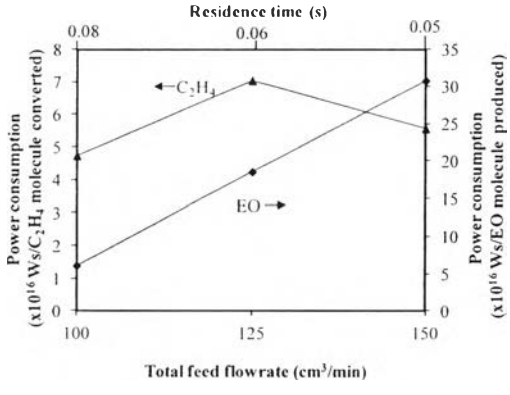

Figure 6.6 (a) C_2H_4 and O_2 conversions and EO yield, (b) product selectivities, (c) power consumption as a function of total feed flow rate (a C_2H_4 feed position of 2 mm, an O_2/C_2H_4 feed molar ratio of 0.5:1, an applied voltage of 18 kV, an input frequency of 500 Hz, and an electrode gap distance of 1 cm).

of the mass flow controllers. The reaction experiments were conducted at a C_2H_4 feed position of 2 mm, an O_2/C_2H_4 feed molar ratio of 0.5:1, an applied voltage of 18 kV, an input frequency of 500 Hz, and an electrode gap distance of 1 cm. Figure 6.6(a) illustrates the influence of the total feed flow rate on the C_2H_4 and O_2 conversions and EO yield. The O_2 conversion markedly decreased with increasing total feed flow rate from 100 to 150 cm^3/min, while the C_2H_4 conversion remained almost unchanged. An increase in the total feed flow rate basically reduces the gas residence time in the reaction system, resulting in having a shorter contact time for C_2H_4 and

O_2 molecules to collide with electrons. Therefore, an increase in the total feed flow rate caused the reduction in the EO yield.

Figure 6.6(b) shows the effect of total feed flow rate on all product selectivities. It can be seen that the EO selectivity decreased significantly with increasing total feed flow rate and it mirrors the EO yield. This is because a higher total feed flow rate reduces the residence time of reactions in the plasma zone, causing lowering the opportunity of collision between oxygen active species and C_2H_4 molecules, thereby decreasing the epoxidation performance. In contrast, the other product selectivities tended to slightly increase with increasing total feed flow rate (i.e. a shorter residence time), suggesting that the ethylene epoxidation is affected more prominently by decreasing residence time as compared to the other reactions.

Figure 6.6(c) shows the effect of total feed flow rate on the power consumptions. The power consumption per molecule of converted C_2H_4 increased with increasing total feed flow rate from 100 to 125 cm^3/min and then decreased with further increasing feed flow rate from 125 to 150 cm^3/min, while the power consumption per molecule of produced EO linearly increased with increasing total feed flow rate throughout the studied feed flow rate range. From the results, the lowest total feed flow rate of 100 cm^3/min was considered as an optimum value in this work since it could provide the highest EO yield, the highest EO selectivity, and the lowest power consumptions.

6.4.6 Effect of Electrode Gap Distance

To investigate the effect of electrode gap distance, the experiments were performed under the best conditions obtained above: a C_2H_4 feed position of 0.2 cm, an O_2/C_2H_4 feed molar ratio of 0.5:1, an applied voltage of 18 kV, an input frequency of 500 Hz, and a total feed flow rate of 100 cm^3/min while the electrode gap distance was varied in the range of 0.8 to 1.2 cm since a large amount of coke filaments was found to deposit on the electrode surfaces at an electrode gap distance lower than 0.8 cm, and the generated plasma became non-uniform at an electrode gap distance higher than 1.2 cm. An increase in electrode gap distance can affect both current and residence time of reactants in the plasma zone which will be discussed

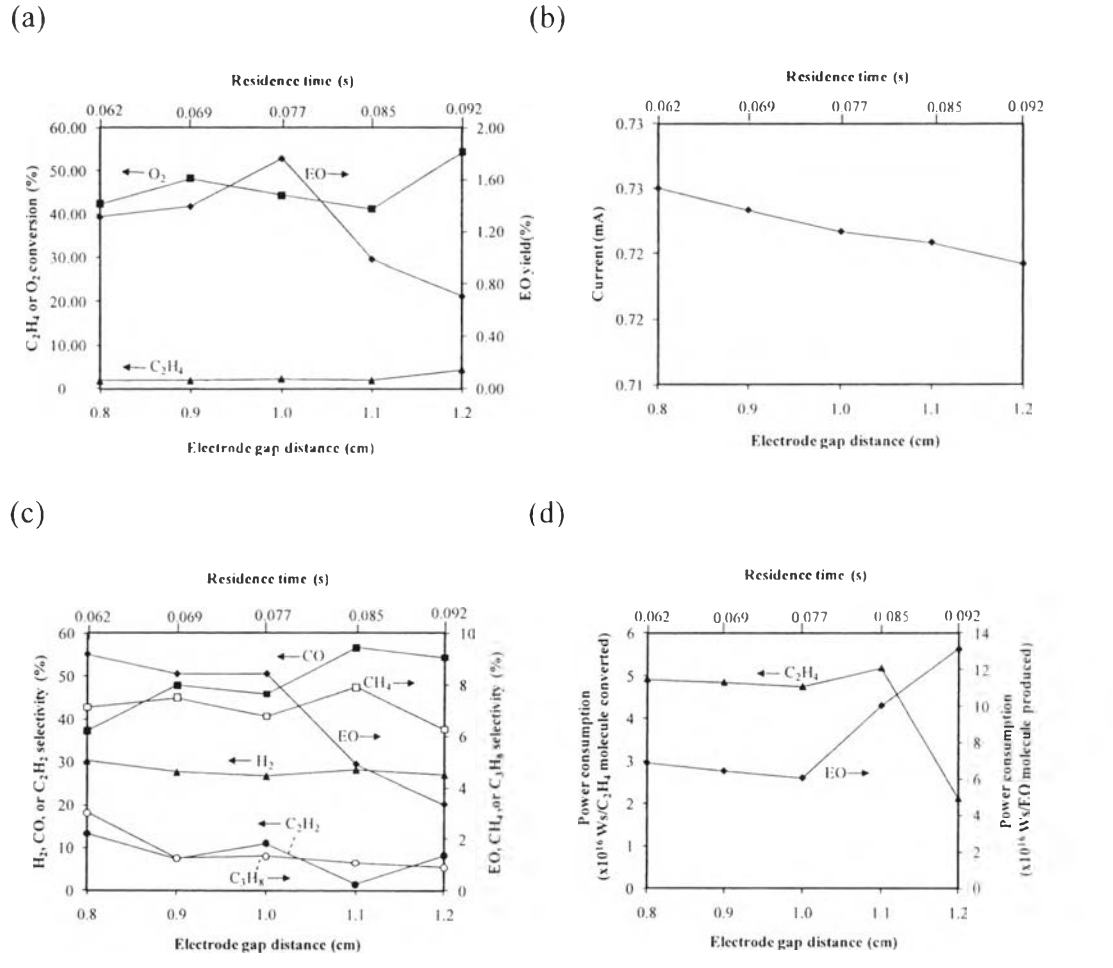

Figure 6.7 (a) C_2H_4 and O_2 conversions and EO yield, (b) generated current, (c) product selectivities, (d) power consumption as a function of electrode gap distance (a C_2H_4 feed position of 0.2 cm, an O_2/C_2H_4 feed molar ratio of 0.5:1, an applied voltage of 18 kV, an input frequency of 500 Hz, and a total feed flow rate of 100 cm^3/min).

later. The effect of electrode gap distance on the C_2H_4 and O_2 conversions and EO yield is illustrated on Figure 6.7(a). The C_2H_4 conversion tended to remain almost unchanged throughout the studied range of electrode gap distance. In contrast, the O_2 conversion fluctuated but tended to increase with increasing electrode gap distance. As shown in Figure 6.7(b), with increasing electrode gap distance, the generated current decreases while the residence time of reactants in plasma zone increases. Interestingly, the EO yield increased with increasing electrode gap distance from 0.8

to 1 cm. Beyond the electrode gap distance of 1 cm, the EO yield decreased markedly with further increasing electrode gap distance. The results suggest that the effect of increasing residence time is more dominant than that of decreasing current.

The effect of electrode gap distance on all product selectivities for EO, CO, H_2, CH_4, C_2H_2, and C_3H_8 is shown in Figure 6.7(c). The EO selectivity tended to remain almost constant in the range of electrode gap distance from 0.8 to 1 cm and then sharply decreased with further increasing electrode gap distance. The selectivities for H_2, CH_4, C_2H_2, and C_3H_8 tended to slightly change with increasing electrode gap distance but the CO selectivity significantly increased with increasing electrode gap distance, which corresponded well to the result of increasing O_2 conversion. The results suggest that the ethylene epoxidation reaction is more pronounced at a shot residence time (or reaction time) but a longer residence time promotes oxidation reaction in which the formed EO is further oxidized to CO. As mentioned before, an increase in electrode gap distance can cause two positive and negative effects of increasing residence time and decreasing current, respectively, affecting the ethylene epoxidation reaction. The optimum electrode gap distance of 1 cm is a trade off of these two effects.

Figure 6.7(d) shows power consumption as a function of gap distance. The power consumption per molecule of converted C_2H_4 tended to slightly vary with increasing electrode gap distance in the range of 0.8 to 1.1 cm and then rapidly decreased with further increasing electrode gap distance from 1.1 to 1.2 cm, whereas the power consumption per molecule of produced EO slightly decreased in the electrode gap distance range of 0.8–1 cm and then sharply increased with further increasing electrode gap distance from 1 to 1.2 cm. A possible reason is that a higher electrode gap distance causes a higher opportunity of secondary reactions, as experimentally evidenced shown in Figure 6.7(c). Therefore, the electrode gap distance of 1 cm was considered to be the optimum value because it provided the highest EO yield, the highest EO selectivity, and the comparatively low power consumption per molecule of produced EO.

6.4.7 Performance Comparisons between Separate and Mixed Feeds of C_2H_4 and O_2

To clearly understand the ethylene epoxidation reaction under the separate and mixed feed conditions in corona discharge, all possible chemical reaction pathways that may occur under the studied conditions are proposed as following equations.

$$O_2 + 2e^- \rightarrow 2O + 2e^- \quad (6.5)$$

$$C_2H_4 + 1/2O_2 \rightarrow C_2H_4O \quad (6.6)$$

$$C_2H_4 + O \rightarrow C_2H_4O \quad (6.7)$$

$$C_2H_4 + 2O \rightarrow 2CO + 2H_2 \quad (6.8)$$

$$C_2H_4 + 2O_2 \rightarrow 2CO + 2H_2O \quad (6.9)$$

$$C_2H_4 + 4O \rightarrow 2CO + 2H_2O \quad (6.10)$$

$$C_2H_4 + O \rightarrow C_2H_3 + OH \quad (6.11)$$

$$C_2H_3 + 2O \rightarrow CO + 3H \quad (6.12)$$

$$C_2H_3 + O \rightarrow C_2H_2 + OH \quad (6.13)$$

$$C_2H_4O + 3/2O_2 \rightarrow 2CO + 2H_2O \quad (6.14)$$

$$C_2H_4O + O \rightarrow 2CO + 2H_2 \quad (6.15)$$

$$C_2H_4O + 3O \rightarrow 2CO + 2H_2O \quad (6.16)$$

$$H_2 + 2e^- \rightarrow 2H + 2e^- \quad (6.17)$$

$$H_2O + 2e^- \rightarrow H + OH + 2e^- \quad (6.18)$$

$$C_2H_4 + 2e^- \rightarrow C_2H_2 + H_2 + 2e^- \quad (6.19)$$

$$C_2H_4 + 2e^- \rightarrow CH_4 + C + 2e^- \quad (6.20)$$

$$C_2H_4O + 2e^- \rightarrow CH_4 + 2CO + 2e^- \quad (6.21)$$

$$C_2H_4 + H \rightarrow C_2H_3 + H_2 \quad (6.22)$$

$$C_2H_3 + H \rightarrow C_2H_2 + H_2 \quad (6.23)$$

$$C_2H_4 + H \rightarrow C_2H_5 \quad (6.24)$$

$$C_2H_4 + 2H + 2e^- \rightarrow 2CH_3 + 2e^- \quad (6.25)$$

$$C_2H_5 + CH_3 \rightarrow C_3H_8 \quad (6.26)$$

$$C_2H_2 + CH_3 + 3H \rightarrow C_3H_8 \quad (6.27)$$

$$CH_3 + H \rightarrow CH_4 \quad (6.28)$$

$$C_3H_8 \rightarrow C_2H_2 + CH_4 \quad (6.29)$$

In this work, the desired reaction is the ethylene epoxidation (equations 6.6 and 6.7), while the other reactions, such as cracking (equations 6.20 and 6.21), dehydrogenation (equations 6.11-13,6.19,6.22, and 6.23), combustion (equations 6.8-6.10,6.14-6.16), and coupling (equations 6.26 and 6.27) can occur in the studied system. To maximize the EO formation with the minima of undesired other products, one has to activate only oxygen molecules to produce oxygen active species to further react with inactivated C_2H_4 molecules, which, in turn, can reduce all undesired other products. The separate feed of C_2H_4 and O_2 with an appropriate feed position of C_2H_4 was hypothesized in the present work to enhance the ethylene epoxidation reaction.

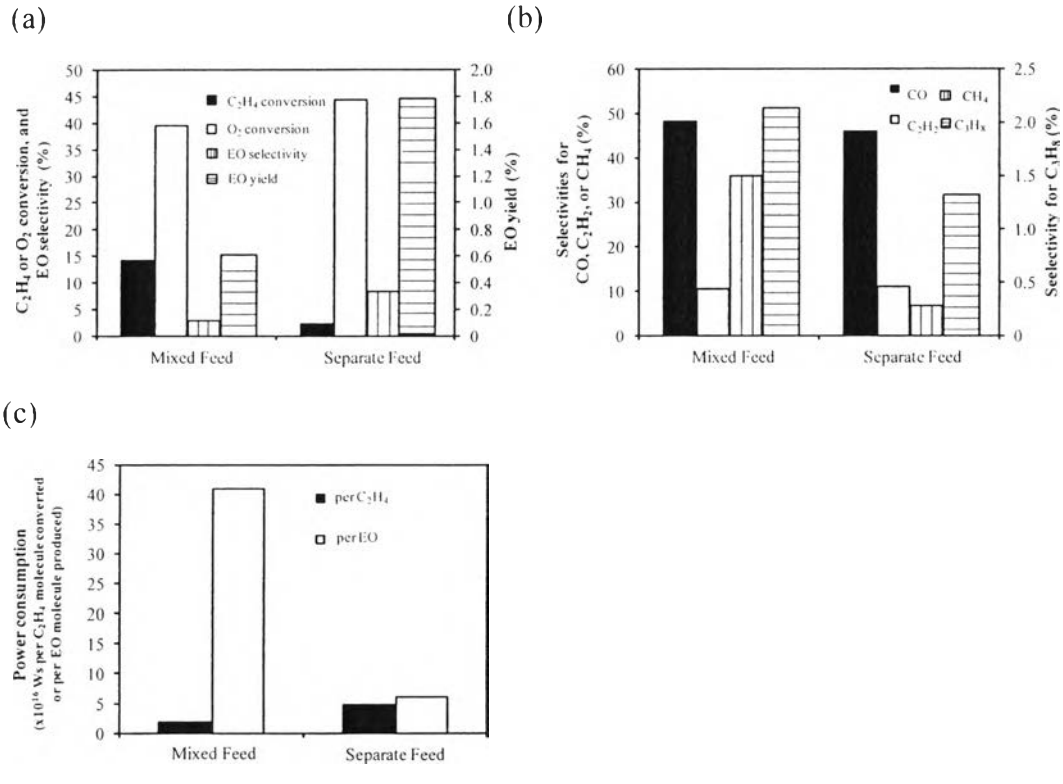

Figure 6.8 Comparisons of the corona discharge performance using the separate and the mixed C_2H_4/O_2 feeds in terms of: (a) C_2H_4 and O_2 conversions, EO selectivity and yield (b) selectivities for other products (c) power consumption under their own optimum conditions [a C_2H_4 feed position of 0.2 (for the separate feed), an O_2/C_2H_4 feed molar ratio of 1:2 (for the separate feed) and 1:1 (for the mixed feed), an applied voltage of 18 kV (for the separate feed) and 15 kV (for the mixed feed), an input frequency of 500 Hz (for both feed systems), a total feed flow rate of 100 (for the

separate feed) and 50 (for the mixed feed) cm^3/min, and an electrode gap distance of 1 cm (for both feed systems)].

The ethylene epoxidation performance of the separate feed and the mixed feed of C_2H_4 and O_2 under their own optimum conditions is shown in Figure 6.8. The optimum conditions for the mixed feed were obtained in our previous work [4]. The system operated with the separate feed gave a higher O_2 conversion than that operated with the mixed feed whereas a much higher C_2H_4 conversion was found in the system with the mixed feed than that with the separate feed (Figure 6.8(a)). Interestingly, it can be clearly seen that the separate feed provided both higher EO selectivity and yield with lower selectivities for other products (CH_4, CO, and C_3H_8) except the C_2H_2 selectivity, as compared to the mixed feed. This is because the separate feed had a lower contact time between the high energetic electrons and C_2H_4 molecules, leading to decreasing the opportunity of all undesired reactions. Consequently, the lower selectivities for CO, CH_4, and C_3H_8 were obtained from the separate feed system (Figure 6.8(b)). The power consumptions per EO molecule produced and per C_2H_4 molecule converted of both the separate and mixed feed systems are comparatively shown in Figure 6.8(c). For the separate feed system, the power consumptions per EO molecule produced was extremely lower, resulting from the high EO yield and selectivity. In contrast, the power consumption per C_2H_4 molecule converted was slightly higher for the separate feed system, as compared with the mixed feed system.

6.5 Conclusions

In this research, the ethylene epoxidation was investigated in low-temperature corona discharge. To enhance the EO selectivity, C_2H_4 was fed at different location of the plasma zone which, in turn, can reduce the opportunity of collision between C_2H_4 molecules and generated electrons, leading to lowering undesired other products as well as increasing EO formation. A C_2H_4 feed position of 0.2 cm was experimentally found to be the most suitable position, providing the highest EO selectivity and yield with the lowest power consumption for one molecule of EO produced. The effects of various operating parameters, including O_2/C_2H_4 feed molar ratio, applied voltage, input frequency, total feed flow rate, and

electrode gap distance, on the epoxidation performance were also investigated in order to achieve the optimum conditions. The separate feed system was found to provide higher EO selectivity and yield with a lower power consumption, as compared with the mixed feed system.

6.6 Acknowledgements

The authors would like to gratefully acknowledge the Dudsadeepipat Scholarship, Chulalongkorn University, Thailand and the Center of Excellence on Petrochemical and Materials Technology, Chulalongkorn University, Thailand.

6.7 References

1. L.M. Zhou, B. Xue, U. Kogelschatz, B. Eliasson, Plasma Chem. Plasma Process 18 (1998) 375-393.
2. F.M. Aghamir, N.S. Matin, A.H. Jalili, M.H. Esfarayeni, M.A. Khodagholi, R. Ahmadi. Plasma Chem. Plasma Process 13 (2004) 707-711.
3. T. Sreethawong, T. Suwannabart, S. Chavadej, Plasma Chem. Plasma Process 28 (2008) 629-642.
4. S. Chavadej, A. Tansuwan, T. Sreethawong, Plasma Chem. Plasma Process 28 (2008) 643-662.
5. T. Sreethawong, N. Permsin, T. Suttikul, S. Chavadej, Plasma Chem. Plasma Process 30 (2010) 503-524.
6. M.R. Khani, S.H.R. Barzoki, M.S. Yaghmaee, S.I. Hosseini, M. Shariat, B. Shokri, A.R. Fakhari, S. Nojavan, H. Tabani, and M. Ghaedian, IEEE T. Plasma Sci. 39 (2011) 1807-1813.
7. Z. Fang, H. Yang, Y. Qiu, IEEE T. Plasma Sci. 38 (2010) 1615-1623.
8. N. De Geyter, R. Morent, T. Jacobs, F. Axisa, L. Gengembre, C. Leys, J. Vanfleteren, E. Payen, Plasma Process Polm. 6 (2009) S406-S411.
9. M. Okubo, M. Tahara, N. Saeki, T. Yamamoto, Thin Solid films 516 (2008) 6592-6597.
10. R.S. Besser, P.J. Lindner, J. Power sources 196 (2011) 9008-9012.
11. R. Burlica, K.Y. Shih, B. Hnatiuc, B.R. Locke, Ind. Eng Chem. 50 (2011) 9466-9470.

12. X. Zhu, T. Hoang, L.L. Lobban, R.G. Mallinson, J. Phys. D: Appl. Phys. 44 (2011) 274002.

13. N. Rueangjitt, C. Akarawitoo, T. Sreethawong, S. Chavadej. Plasma Chem. Plasma Process 27 (2007) 559-576.

14. Y.N. Chun, H.O. Song, Environ. Eng. Sci. 23 (2006) 1017-1023.

15. W.J. Liang, H.P. Fang, J. Li, F. Zheng, J.X. Li, Y.Q. Jin, J. Electrostatics 69 (2011) 206-213.

16. J. Jarrige, P. Vervisch, Plasma Chem. Plasma Process 27 (2007) 241-255.

17. D.J. Helfritch, IEEE T. Ind. Appl. 29 (1993) 882-886.

18. G.B. Zhao, S. Joh, , J.J. Zhang, J.C. Hamann, S.S. Muknahallipatna, S. Legowski, J.F. Ackerman, M.D. Argyle, Chem. Eng. Sci. 62 (2007) 2216-222

19. H. Than Quoc An, T. Pham Huu, T. Le Van, J.M. Cormier, A. Khacef, Catal. Today 176 (2011) 474-477.

20. D. Dobrynin, A. Wu, S. Kalghatgi, S. Park, N. Shainsky, K. Wasko, E. Dumani, R. Ownbey, S. Joshi, R. Sensenig, A.D. Brooks, Plasma Med. 1 (2011) 93-108.

21. B. Eliasson, U. Kogelschartz, IEEE T. Plasma Sci. 19 (1991) 1063-1077.

22. T. Sreethawong, T. Suwannabart, S. Chavadej, Chem. Eng. J. 115 (2009) 396-403.

23. T. Suttikul, T. Sreethawong, H. Sekiguchi, S. Chavadej, Plasma Chem. Plasma Process 31 (2011) 273-290.

24. Agency for Toxic Substances and Disease Registry (ATSDR). Toxicological Profile for Ethylene Oxide. U.S. Public Health Service, U.S. Department of Health and Human Services, Atlanta, GA. 1990

25. Y. Jun, D. Jingfa, Y. Xiaohong, Z. Shi, Appl. Catal. A: Gen. 92 (1992) 73-80.

26. S.N. Goncharova, E.A. Paukshtis, B.S. Bal'zhinimaev, Appl. Catal. A: Gen. 126 (1995) 67-84.

27. S. Linic, M.A. Barteau, J. Am. Chem. Soc. 126 (2004) 8086-8087.

28. J.T. Jankowiak, M.A. Barteau, J. Catal. 236 (2005) 379-386.

29. J.C. Dellamorte, J. Lauterback, M.A. Barteau, Catal. Today 120 (2007) 182-185.

30. D. Torres, F. Illas, R.M. Lambert, J. Catal. 260 (2008) 380-383.

31. J.C. Dellamorte, J. Lauterbach, M.A. Barteau, Ind. Eng. Chem. Res. 48 (2009) 5943-5953.